Turbulence Parameters in a Stirred Tank

A. S. MUJUMDAR[1], B. HUANG, D. WOLF[2], M. E. WEBER and W. J. M. DOUGLAS
Department of Chemical Engineering, McGill University, Montreal, Quebec

Mean and fluctuating radial velocities have been measured in the impeller stream of a baffled, turbine-agitated cylindrical tank. Auto-correlation functions, energy spectra and amplitude probability density functions of the radial velocity fluctuations were also obtained. In the vicinity of the impeller, the motion is distinctly periodic, with a time scale corresponding to $n_bN/60$, where n_b is the number of turbine blades and N is the rpm. The amplitude of the periodic component was found to decrease with radial distance from the impeller tip and was used to correct the measured turbulence intensities.

On a mesuré les vélocités radiales moyennes et fluctuantes d'un courant agité dans un réservoir cylindrique décalé et muni de turbine. On a aussi calculé les fonctions d'auto-corrélation, les spectres d'énergie et les fonctions décrivant le degré probable d'amplitude des fluctuations des vélocités radiales. Au voisinage de l'agitateur, le mouvement est distinctement périodique et l'échelle de temps correspond à $n_bN/60$, où n_b est le nombre de lames de la turbine et N est le nombre de tours à la minute. On a trouvé que l'amplitude de l'élément responsable de la périodicité décroissait avec la distance radiale à partir du bout des lames de l'agitateur et l'on a utilisé la dite amplitude pour corriger les intensités mesurées de la turbulence.

Stirred tanks are widely used in the chemical industry for effecting mixing, but their design has so far been empirical. A theoretical treatment of the flow within a stirred tank is rendered intractable by the inherent randomness and three-dimensionality of the flow and non-linearity of the governing equations of motion. Experimental studies of the large- and small-scale turbulence characteristics in stirred vessels may be expected to lead to formulation of realistic models of the flow. These models can then be used to predict such quantities of engineering interest as the mixing efficiency, pumping capacity, power requirements, etc. It was the objective of this work to measure the turbulence characteristics of the high speed stream issuing from a turbine type impeller in a fully baffled tank. Turbulence parameters were measured using a constant-temperature hot-wire anemometer with air as the fluid within the tank. The hot-wire technique was chosen because of the ease of operation and extremely good frequency response.

Use of air as working fluid

Cooper[1] recently showed that the temporal mean velocity distribution in the impeller stream is the same with air and water as the fluid in the tank. We have assumed that the small-scale turbulence characteristics would also be similar at equal Reynolds numbers irrespective of the fluid in the tank. There exists sufficient confirmation in the literature for air and water flows in circular pipes and circular jets, and also grid-generated turbulent flows in wind and water tunnels. Chuang and Cermak[2] have compared their measurements of turbulent intensities, shear stress and energy spectra in the pipe flow of distilled water for a Reynolds number of 5×10^4 with those of Sandborn[3] and Laufer[4] who studied the flow of air in a pipe at the same Reynolds number. The agreement between the air and water data is remarkable despite the totally different techniques of measurement; the former inferred the turbulence characteristics from measured electrokinetic-potential fluctuations while the latter authors used hot-wire anemometers. Martin and Johanson[5] measured turbulence intensities and integral scales by the auto-correlation technique for water turbulence in a pipe for Reynolds numbers of 1.9×10^4 to 1.6×10^5. They compared their results with those of Sandborn[3] in the same Reynolds number range and found satisfactory agreement. Wells, Harkness and Meyer[6], in their work on the turbulent pipe flow of a drag-reducing non-Newtonian fluid, observed that the variation of turbulence intensity, normalized with either local mean velocity or shear velocity, with Reynolds number at the tube centerline for a 0.05 per cent solution of sodium carboxymethyl cellulose (CMC) in water, water, and air is the same. They also showed that the non-dimensionalized spectra for water agreed fairly well with the air spectra[4].

Fabula[7] arrived at the conclusion that good agreement exists between the spectra for air and water flows through pipes, when these are normalized with respect to dissipation variables. At a sufficiently large turbulence Reynolds number Re_T, he showed that the function $E_1(k_1/(\epsilon\nu^5)^{1/4}$ is a universal function of k_1/k_d, where $E_1(k_1$ is the one-dimensional spectrum function, ϵ is the dissipation rate, k_d is the Kolmogoroff wave number and ν is the kinematic viscosity. It is thus possible to calculate the effect of a change in fluid viscosity on the spectrum as long as the fluid is Newtonian. Scaling techniques for non-Newtonian fluids do not now exist.

Bankoff and Rosler[8,9] used a constant-temperature hot-film anemometer to obtain mean velocity distributions, intensities and scales of turbulence, and the spectral energy distributions in a water jet. Their results compared very well with the air jet data of

[1]Present address: Carrier Corporation, Syracuse, N.Y.
[2]Present address: Weizmann Institute of Science, Rehovoth, Israel.

Corrsin and Uberoi[11]. Grid-generated turbulence spectra in air as obtained by Comte-Bellot and Corrsin[12] and those in water as measured by Fabula[9] showed very good agreement. Also, the viscous dissipation rates and dissipation spectra were found to compare well.

In view of the above, it was assumed that this similarity would hold in the case of the impeller stream of a turbine-agitated tank. This assumption effects a tremendous simplification in the measurement procedure as the hot-wire is more accurate than the hot-film probe which presents problems in maintaining a non-drifting calibration and in achieving good high-frequency response.

Review of earlier work on stirred tank turbulence

Manning and Wilhelm[13] measured concentration fluctuations with a conductivity probe. Assuming a normal distribution of the fluctuating velocity and its time derivative, and no correlation to exist between the two, they obtained unrealistically large values for the micro-scale, possibly for two reasons. First, the normality assumptions are dubious in the high turbulent intensity shear flow which exists in the impeller stream and secondly, the use of a strip-chart pen recorder effectively precludes any possibility of picking up the high frequencies associated with the dissipation scale without frequency transformation of the fluctuating signal.

Similar measurements were made with a smaller probe by Reith[14]. He found that the spectrum of concentration fluctuations contained a Kolmogoroff -5/3 wave number region and that the spectra were not similar at a fixed position for several impeller speeds. Reith also reports integral concentration scales of the order of twice the impeller diameter, values which seem unrealistically large. His results lead to the important conclusion that the principle of Reynolds number similarity predicts correctly the influence of impeller speed on the turbulence decay rate.

Kim and Manning[15] measured the radial components of the turbulence energy within a stirred, baffled tank with a piezo-electric transducer probe. They could not determine the absolute levels of the intensity due to a limitation on their technique. Results of their spectral measurements over the frequency range of 19 to 1,100 Hz indicated that the energy spectra were proportional to $k^{-10/3}$ over one decade. The spectra were similar above a wave number of 80 ft^{-1} for all radial positions.

Perhaps the first attempt to describe the fluid flow phenomena in stirred liquids using hot-wire technique was made by Bowers[16]. He measured the tangential and vertical velocities, turbulence intensity and eddy diameter distributions in various Newtonian liquids. The types of agitators used included two-bladed paddles and multi-bladed turbines with both vertical and inclined blades. His results indicated that the tangential and vertical velocities can be expressed as a constant factor of the tip speed and, more importantly, this fraction is substantially independent of scale for geometrically similar systems. However, the turbulence intensity relative to the tip speed was found to change for geometrically similar systems.

Schwartzberg and Treybal[17] report measurements of mean and rms velocities obtained by photographing small neutrally buoyant particles stirred in water. At a position above the impeller and outside the high velocity impeller stream they find that the mean and fluctuating velocities are proportional to ND^2, thus suggesting that U_{TIP} is not a good velocity scaling parameter. No data are given on the length of exposure used in obtaining the streak photographs.

Cutter[18] used the photographic technique to obtain Eulerian correlation coefficients in addition to the mean and fluctuating velocities of water in a fully baffled stirred tank. The data were confirmed using a Kiel impact tube. His technique involved photographing lycopodium particles with an exposure short enough so that the particles showed up as short streaks in the picture. The exposure time was 1/600 sec. Recently, he applied the same technique to study the non-random velocity fluctuations caused by the motion of the impeller blades in a baffled tank[19]. His results indicate that the non-random component decays as it proceeds towards the wall. Assuming no other limitations on this technique, it is immediately obvious that its upper frequency limit is no higher than 300 cps. It may be noted that although the light technique allows evaluation of the correlation function, it cannot be used to obtain the energy spectrum directly. Fourier-transformation of the correlation function in a "non-frozen" pattern of turbulence to obtain the spectrum is subject to uncertainty without knowledge of the convection velocity. An important aspect of Cutter's work[18] was the determination of local rates of energy dissipation. According to Kolmogoroff's theory[20] of local isotropy, the small-scale eddies are isotropic at sufficiently large Reynolds numbers and hence are independent of the structure of the larger eddies and the mechanism of their generation. The intensity of the small-scale eddies is dependent only on the local rate of energy dissipation and the viscosity of the fluid. The distribution of the local rates of energy dissipation could be a useful criterion of mixing, as pointed out by Cutter[18].

Definitions of measured quantities[20, 21]

The instantaneous velocity, U_i, in a turbulent flow can generally be expressed as

$$U_i = \overline{U}_i + u_i \quad (i = 1,2,3) \qquad (1)$$

where $\overline{U}_i$ is the time-mean velocity and u_i is the instantaneous fluctuating velocity in the i-direction. The relative intensity of turbulence, I, is defined as

$$I = \frac{u'}{\overline{U}} \qquad (2)$$

where u' is the temporal root-mean-square value of the fluctuating velocity.

Spectrum of turbulence

The random velocity fluctuations, u_i, can be Fourier-analyzed into their harmonic components of various scales. The energy contributions of the fluctuations of different frequencies can thus be obtained and presented in the form of a frequency spectrum. Conventionally, the turbulence spectra are represented in the wave number space rather than in the frequency domain. Frequency, f, and wave number, k, are related by the equation

$$k = 2\pi f/U_c \qquad (3)$$

where U_c is the convection velocity, i.e. the velocity at which the turbulence pattern is swept past the stationary point of observation. For a "frozen" pattern of turbulence which exists when the turbulence level is low, viscous forces are negligible and the mean shear is small, $U_c = \overline{U}$ (Taylor's hypothesis). It should be noted that the wave number space is three-dimensional and hence the theoretical spectrum function is a tensor of rank two. The measured spectrum func-

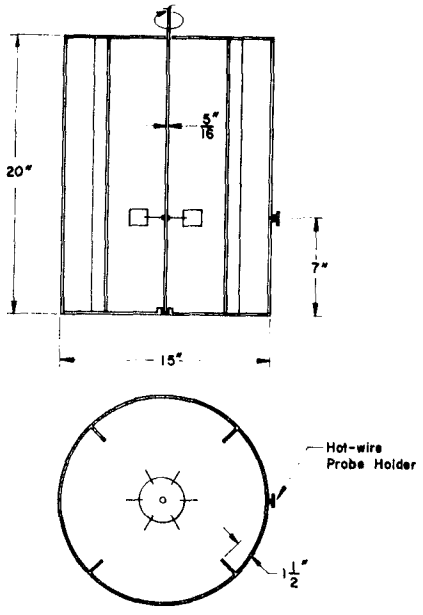

Figure 1 – Tank and impeller assembly.

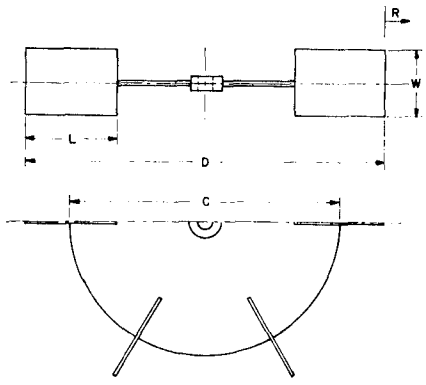

Figure 2 – Dimensions of turbine-type impellers.

DIAMETER D in.	BLADE WIDTH in.	BLADE LENGTH in	DISK DIA. in.	NO. OF BLADES
5	1	2	3 1/4	6
6	1	2 1/4	3 3/4	6

tion is, however, one-dimensional and the two are related exactly only for homogeneous and isotropic turbulence. Nevertheless, it is possible to give a physically meaningful interpretation of the one-dimensional spectrum $E_1(k_1)$, which is defined such that $\overline{u^2}\,E_1(k_1)$ is the contribution of wave numbers in the region k_1 and k_1+dk_1 to the total turbulence energy. Hence,

$$\int_0^\infty E_1(k_1)dk_1 = 1.0 \quad \ldots\ldots(4)$$

The subscript $_1$ refers to the fact that the measured spectrum function is one-dimensional.

Dissipation spectrum

The dissipation spectrum is determined as a function of wave number from

$$\phi_1(k_1) = k_1^2 E_1(k_1) \quad \ldots\ldots(5)$$

Auto-correlation function

The auto-correlation function $R(\tau)$ is defined as

$$R(\tau) = \frac{\overline{u(t)u(t+\tau)}}{\overline{u^2}} \quad \ldots\ldots(6)$$

If we visualize the velocity fluctuations as the result of heterogeneously composed eddies carried along by the mean flow, then there can be distinguished by their role in the energy-cascade process two types of eddies, each characterized by a length scale. An integral scale Λ_R, is defined as

$$\Lambda_R = U_c \int_0^{\tau_0} R(\tau)d\tau \quad \ldots\ldots(7)$$

where τ_0 is generally taken as the time at which $R(\tau)$ first becomes zero. An alternative method of evaluating the integral scale is from the zero frequency intercept of the spectrum function. Assuming Taylor's hypothesis

$$\Lambda_E = \frac{\bar{U}E_1(0)}{4} \quad \ldots\ldots(8)$$

A measure of the smallest eddies can be found from the maximum in the dissipation spectrum. The inverse of the wave number at which the maximum occurs may be taken as a measure of the dissipation eddy scale.

Probability density function (PDF)

The probability density function, $P(u)$, is defined so that $P(u)du$ is the probability that the fluctuating velocity component lies between u and $u+du$. Hence

$$\int_{-\infty}^{\infty} P(u)du = 1.0 \quad \ldots\ldots(9)$$

For homogeneous and isotropic turbulence, the PDF is very nearly Gaussian[22]. Departure from Gaussian bell shape is noted in high shear flows[23,24,25,26]. Theoretical treatments of the statistical theories of turbulence often make the assumption of normality or near-normality of the turbulent velocity for mathematical simplification.

Experimental apparatus and procedures

The turbulence measurements were made in a 15-in. I.D. x 20-in. baffled acrylic tank (baffles 1.5-in.) fitted with a turbine type impeller. Details of the tank assembly are shown in Figure 1. The dimensions of the impellers used are given in Figure 2. The tank was fitted with a cover having a small central hole through which the agitator shaft passed. The impeller was positioned seven inches from the bottom of the tank. The velocity was measured in the horizontal plane at the center of the impeller. The wire was oriented in this plane perpendicular to the radial direction. All traverses were made midway between two baffles.

The mean velocity and turbulence measurements were made using a DISA type 55A01 constant temperature hot-wire anemometer with type 55A25 hot-wire probes. The probe was a platinum-coated tungsten wire, 0.005-mm. diameter and 1-mm. long. A low-pass filter of 20 KHz built into the anemometer circuit was used to discard the electronic noise. The probe was calibrated before and after every run using a DISA type 55A60 calibration unit. The background turbulence of this unit was less than 0.15% at a flow rate of 300 fps. The anemometer was operated at an over-heat ratio of 1.8 so that no corrections were necessary for small variations in ambient temperature. The frequency response of the anemometer was always found to be such that its 3 db down point was over 8 KHz which is much higher than the highest frequency of interest.

The bridge voltage (dc) from the anemometer was fed to a voltage - to - frequency converter and then to an electronic counter to obtain a 5-digit display. Generally 10 second averages were taken since occasional checks against 100 second averages showed no significant difference. The rms voltage corresponding to the fluctuating velocity was

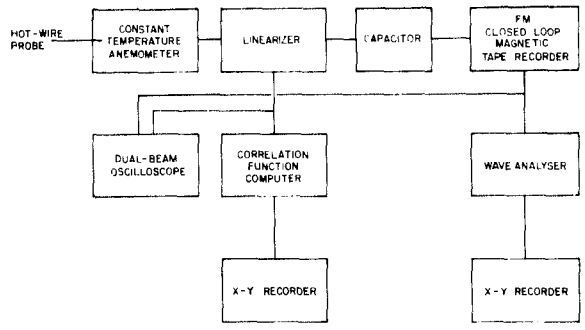

Figure 3 – Schematic circuit diagram for auto-correlation and spectrum analysis.

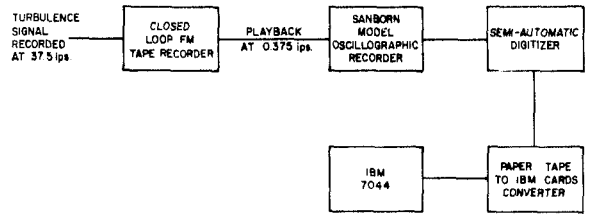

Figure 4 – Schematic flow diagram for digital computation of amplitude probability density and auto-correlation.

read on the true rms meter of the anemometer.

Figure 3 shows the set-up used for spectral analysis and auto-correlation. The turbulence signal from the anemometer was passed through a capacitor to remove the dc bias and then recorded on a 20 ft. magnetic tape loop in the FM (frequency modulated) mode at 37.5 ips. using a PI6102 instrumentation grade tape recorder. The signal was observed visually on an oscilloscope and was also recorded on a strip-chart after frequency transformation, i.e. playing back the recorded signal at a tape speed of 0.375 ips into either a Brush Mark II strip-chart recorder or a Sanborn oscillographic recorder. Both recorders had a flat frequency response up to 100 Hz so that the real time (before slowing down the tape for playback) frequency response was flat over dc to 10,000 Hz.

The amplitude spectra were obtained with a Quan-Tech Model 304 low frequency Wave Analyzer and the energy spectra computed therefrom. The frequency range covered was from 1 Hz to 1 KHz and was analyzed in two stages: the bandwidth 1 Hz to 100 Hz was swept very slowly with narrower filters (1 Hz) and the range 1 Hz to 1 KHz was swept faster with 10 Hz bandwidth filters. Thus spectra with high resolution at low frequencies and uniform statistical accuracy over the entire bandwidth of interest were obtained.

The auto-correlation functions were obtained in real time using a PAR Model 100 correlation function computer manufactured by Princeton Applied Research Corporation. It was used in the AC-coupled mode to block the large bias in the turbulence output signal from the anemometer. The AC coupling forms a high-pass filter, the three db down point of which is 0.32 Hz when autocorrelating. The correlogram was observed on an oscilloscope and also recorded on an X-Y recorder. The upper frequency limit of the computer was well above the highest frequency of interest in this work at all time delay ranges used. The averaging time constant was factory-adjusted at 20 seconds which is large compared with the large scale periodicity of the flow even at the lowest rpm. The time accuracy is within $\pm$ 2%. The correlograms were digitized and replotted to appropriate scales on a Calcomp 565 digital plotter after appropriate computer processing.

The auto-correlation and amplitude probability density functions were computed digitally, as shown schematically in Figure 4. The turbulence signal was recorded on a strip-chart speed of 125 mm/sec after slowing down the taped signal by a factor of 100. The chart recording was digitized at intervals of 1/10 inch on a semi- automatic digitizer designer and built by the Pulp and Paper Research Institute of Canada. The digitizer is accurate to within two-thousandths of an inch and gives a paper tape which was then converted into IBM cards for processing on a computer.

RESULTS AND DISCUSSION

The signal from the hot wire anemometer is shown in Figure 5 for a 6-in. turbine at 600 rpm. Figure 5a shows the signal ¼-in. from the turbine. Succeeding figures show the wire output at ½, ¾, 1, and 2-in. from the impeller. The large periodic component is to be noted. The average period is 60 cps indicating that this periodicity is produced by the passing of the six blades.

Mean velocity profile

The variation of mean radial velocity with distance is shown in Figure 6 for the 6-in. impeller at several rpm. The velocities have been normalized with the velocity of the impeller tip. The trends shown are in agreement with those of earlier workers[16,18].

As shown by Kim and Manning[18] for axisymmetric flow in the center plane of the impeller, a log-log plot of $\overline{U}/U_{TIP}$ versus ρ should have a slope of -1. Data plotted according to this test are shown in Figure 7. Axisymmetry is exhibited over the middle range of ρ values with more complicated flow patterns very close to the turbine and near the walls.

Fluctuating velocity components

The rms value of the fluctuating velocity is plotted in Figure 8 as a function of position for the 6-in. turbine at two rpm values. A local maximum is exhibited some distance from the impeller with the values when decreasing toward the wall. The same data are replotted as local intensity of turbulence in Figure 9. Intensities in the range 35-60% predominate, with some decrease in intensity with impeller speed. It may be noted that the local intensity of turbulence actually increases with distance from the impeller tip because the mean velocity decreases in this direction somewhat more rapidly than does the rms fluctuating velocity.

Spectrum of turbulence

The one dimensional energy spectra are shown in Figures 10 and 11, as a function of frequency up to 1000 Hz. The analysis was not carried further as in all cases the energy content at higher frequencies was less than 5%. Near the impeller (Figure 10) a sharp peak is seen at frequency.

$$f_t = n_b N/60 \quad \ldots\ldots\ldots\ldots\ldots\ldots\ldots\ldots (10)$$

corresponding to the passage of the blades. A smaller peak is also seen at the first harmonic, $2f_t$. Farther away from the impeller (Figure 11) the sharp peak disappears, with that at the harmonic being more persistent. No Kolmogoroff -5/3 range was observed, possibly due to the presence of the non-random component. As the wall is approached, the spectra become similar.

It would have been instructive to compare the spectrum obtained with air in the present study with that for water from the study of Kim and Manning[15]. However, this could not be done, reliably, because of errors noted in that publication and also lack of some of the data needed.

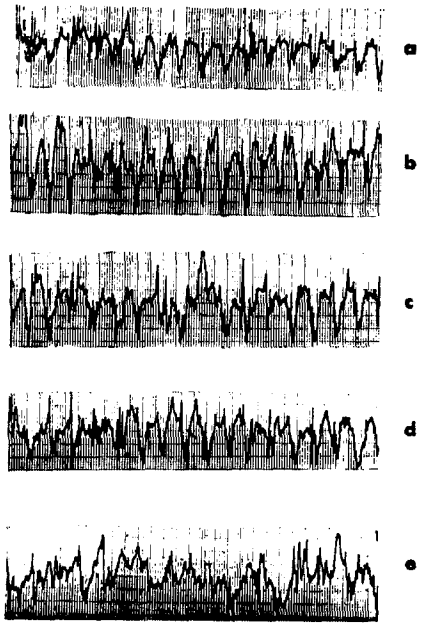

Figure 5 – Hot-wire signals at different radial distances for 6-in. turbine at 600 rpm. a. R = ¼-in., b. R = ½-in., c. R = ¾-in. d. R = 1-in. and e. R = 2-in. (Scale: 1 division = 2 msec in real time).

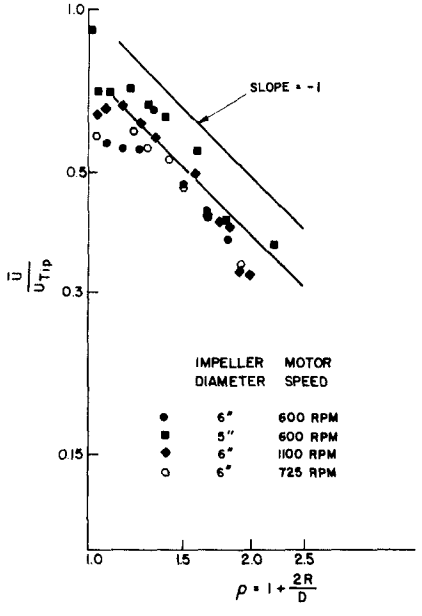

Figure 7 – Check for axi-symmetry of the flow in impeller stream.

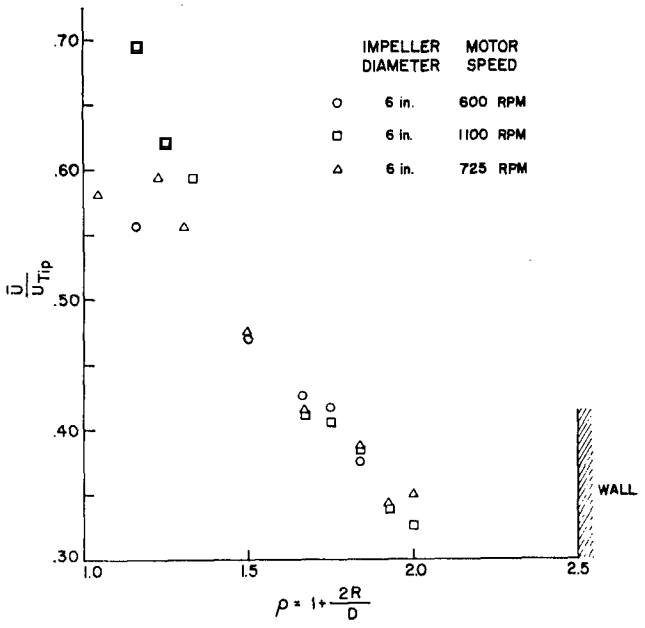

Figure 6 – Non-dimensional mean velocity distribution.

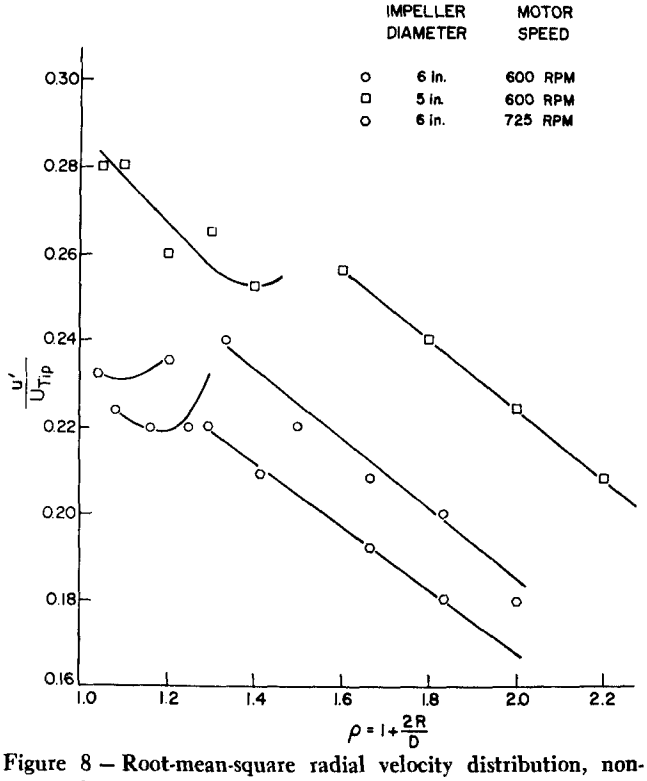

Figure 8 – Root-mean-square radial velocity distribution, non-dimensionalized with respect to the tip velocity.

The dissipation spectra are shown in Figures 12 and 13. They show a peak at the turbulence generating frequency of 60 Hz near the impeller, and a second peak at about 150-200 Hz near the wall. This latter peak is believed due to the eddies responsible for the dissipation of turbulent energy. The energy dissipation rates could not be calculated from these data as the spectral analysis was not extended beyond 1000 Hz. However, it appears that the rate of dissipation increases with distance from the impeller and then decreases near the wall.

Correlation coefficient

A representative correlation coefficient is shown in Figure 14. The coefficient is strongly periodic near the impeller with the periodic component decreasing with distance until no periodicity is evident 2 in. from the turbine. Curves of similar shape were obtained at other rpm with the periodicity disappearing nearer the impeller the lower the rpm.

If it is assumed that the velocity is made up of a periodic component upon which is superimposed a random velocity fluctuation and that the periodic and random components are uncorrelated, then

$$R(\tau) = Ke^{-\alpha\tau} + \frac{A^2}{2}\cos\omega\tau \quad \ldots\ldots\ldots\ldots (11)$$

where α is a measure of the bandwidth of the noise, A is the amplitude of the sine wave, and ω is the angular frequency of the sine wave.

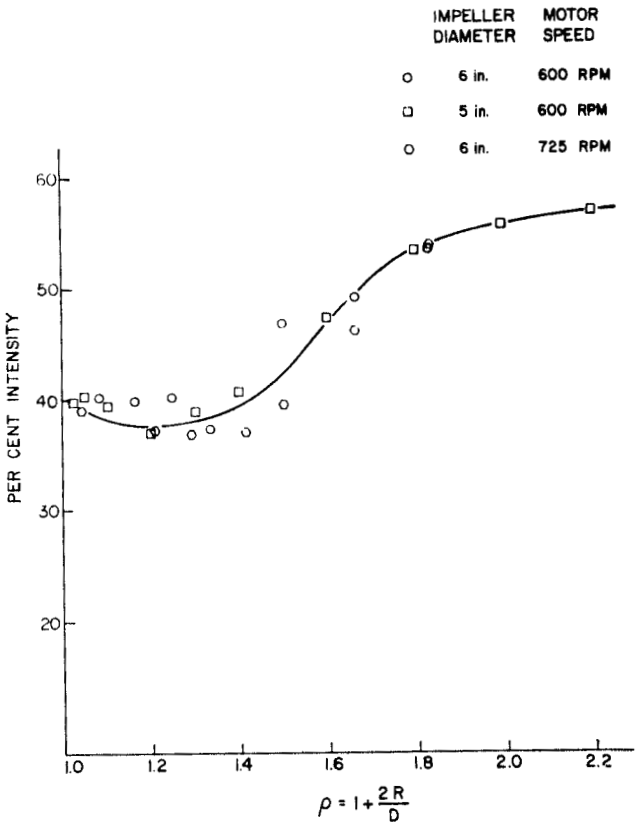

Figure 9 – Relative intensity distribution.

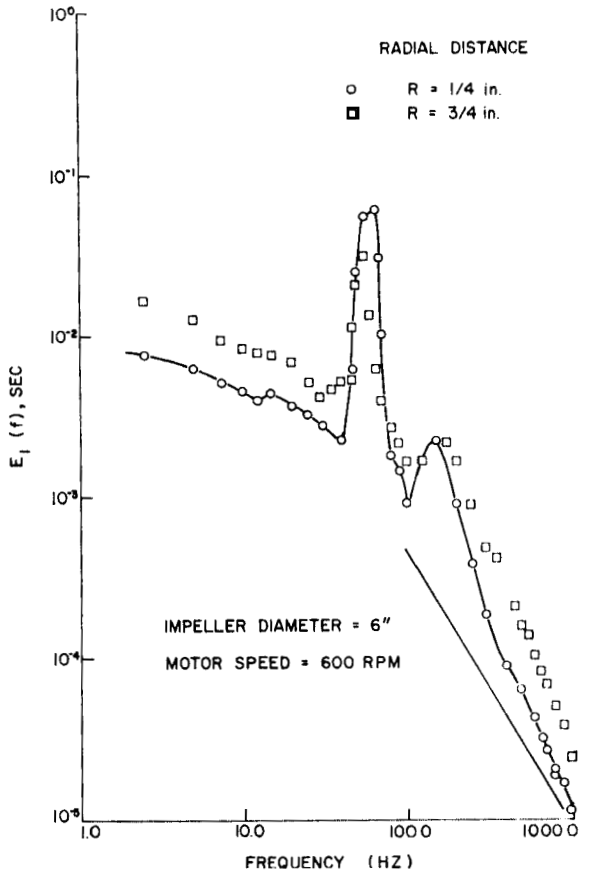

Figure 10 – One-dimensional frequency spectrum of radial velocity fluctuations at R = ¼-in. and ¾-in.

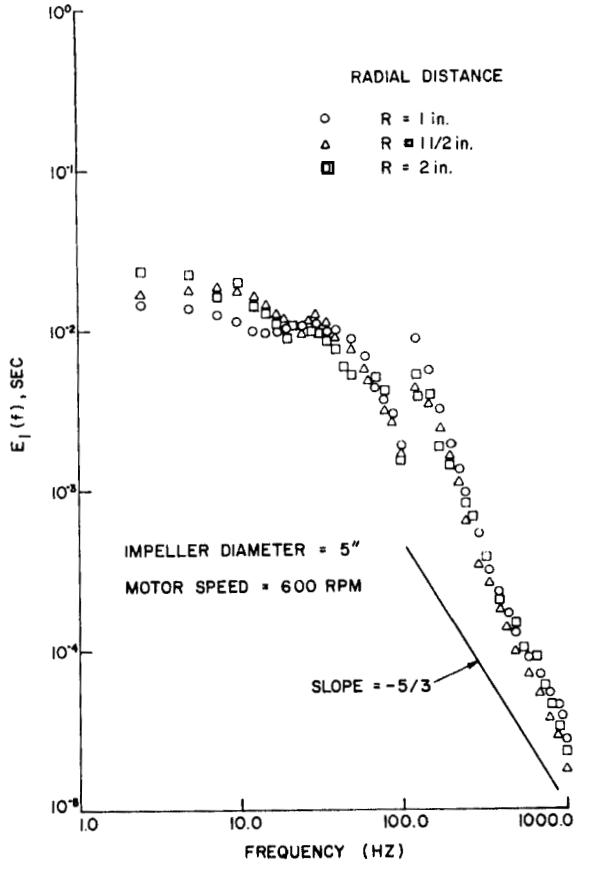

Figure 11 – One-dimensional frequency spectrum of radial velocity fluctuations at R = 1-in., 1½-in. and 2-in.

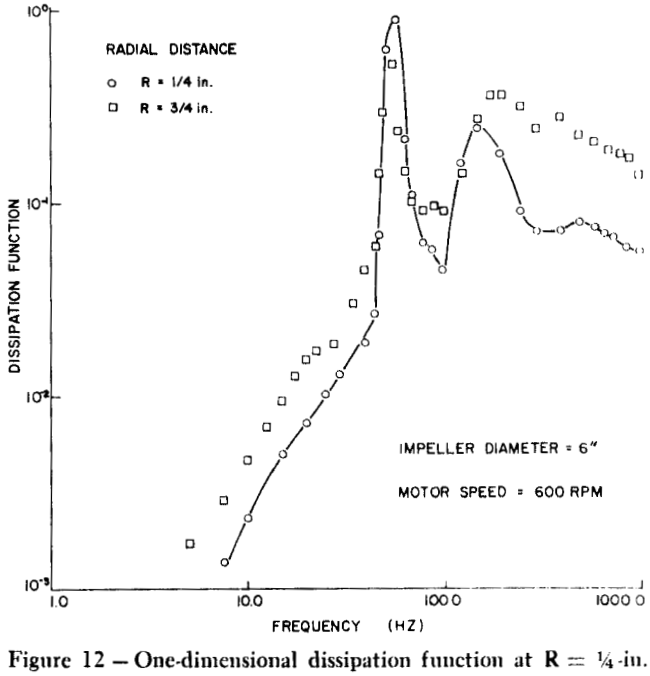

Figure 12 – One-dimensional dissipation function at R = ¼-in. and ¾-in.

The rms value of the random noise, K, can be determined from the correlation coefficient and thus a corrected or true turbulence intensity can be found. These corrected intensities are plotted in Figure 15 along with the original data, some of which is shown in Figure 9. The corrected intensities are lower near the impeller than the raw data, with the data for both rpm's lying on the same curve. Although the above

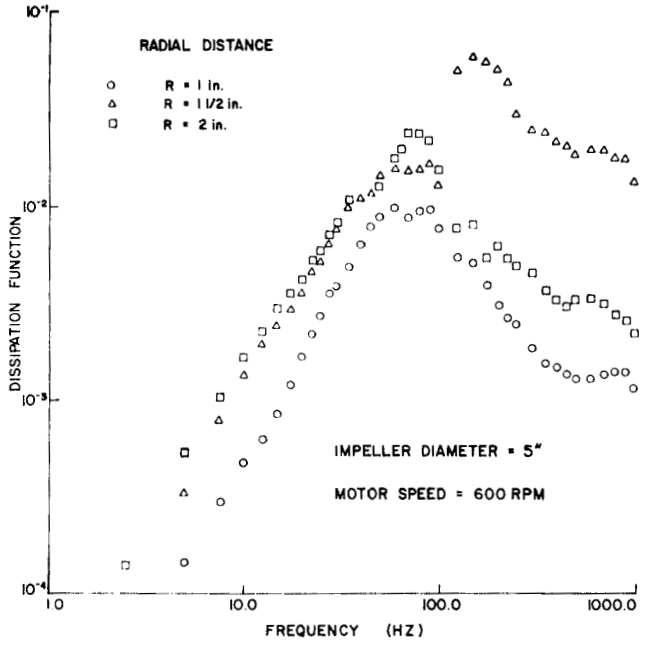

Figure 13 – One-dimensional dissipation function at R = 1-in., 1½-in. and R = 2-in.

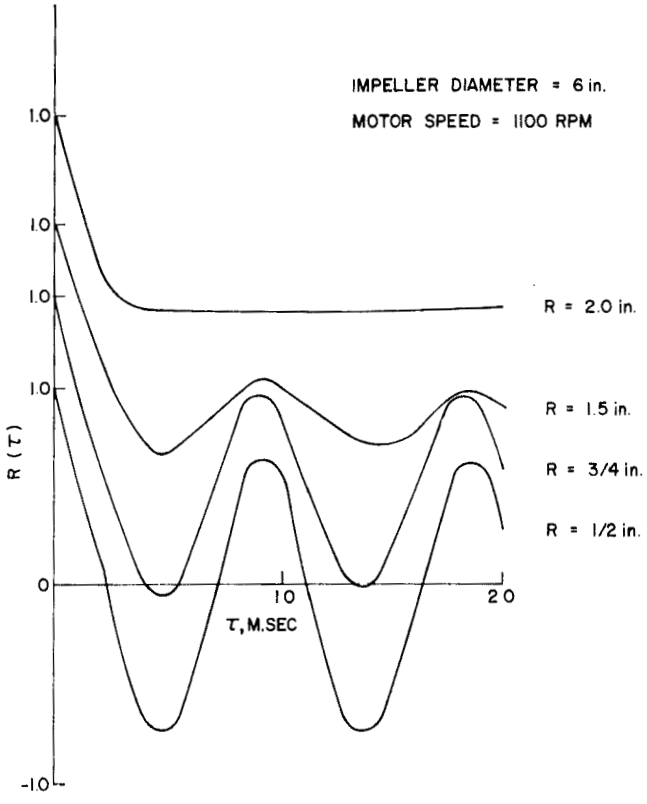

Figure 14 – Auto-correlograms for 6-in. diameter impeller at 1,100 rpm.

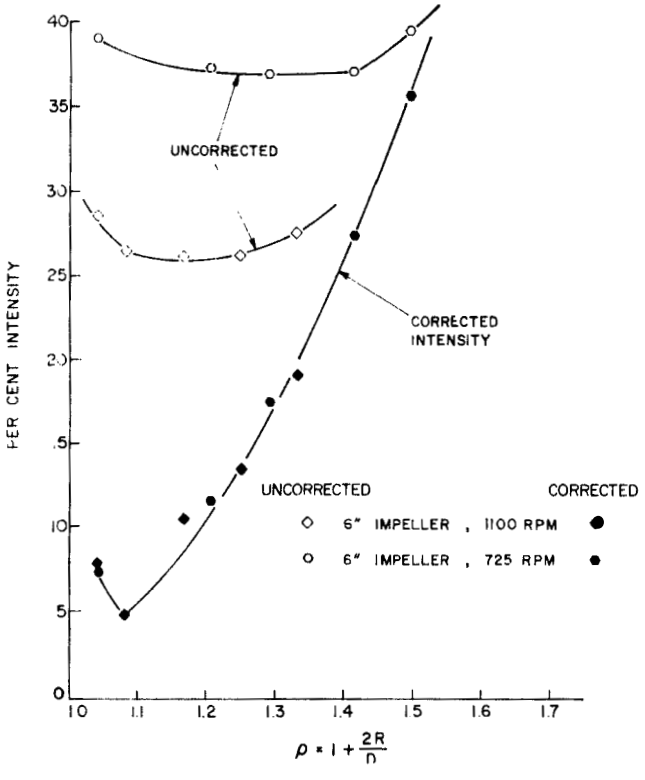

Figure 15 – Comparison of relative turbulence intensity corrected for periodicity with the uncorrected intensities.

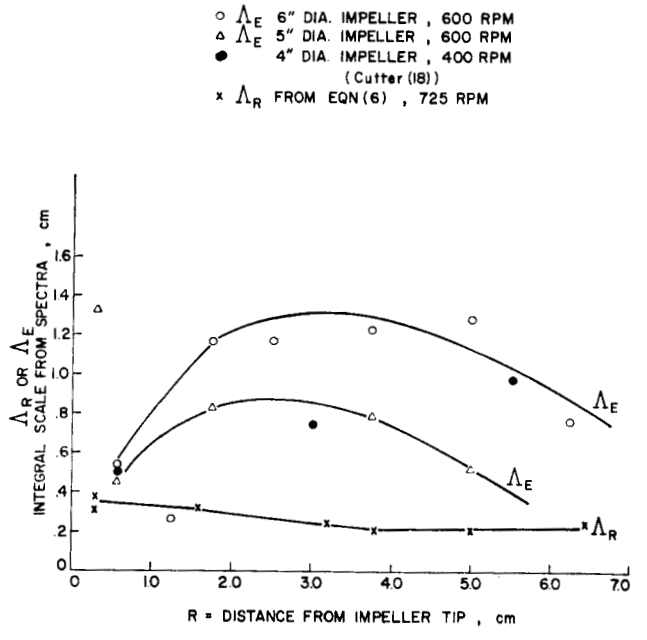

Figure 16 – Variation of integral scales of turbulence with radial distance from the tip.

assumptions are not strictly valid, the corrected intensities as calculated do provide a much better indication of the microscopic turbulence structure in the impeller stream flow.

Scales of turbulence

The macroscale, Λ_R, was computed from the correlation coefficient using Equation (7) and is plotted against radial distance in Figure 16. The macroscale was also calculated from the spectra using Equation (8) yielding Λ_E. This scale should provide an estimate of the eddy size unbiased by the large periodic fluctuations produced by the passage of the turbine blades. This procedure is reasonably accurate here as the spectra were determined down to a frequency of 2 Hz. The results are shown in Figure 16 along with Cutter's[18] data. The scales determined from the spectra and those of Cutter are of the same magnitude and

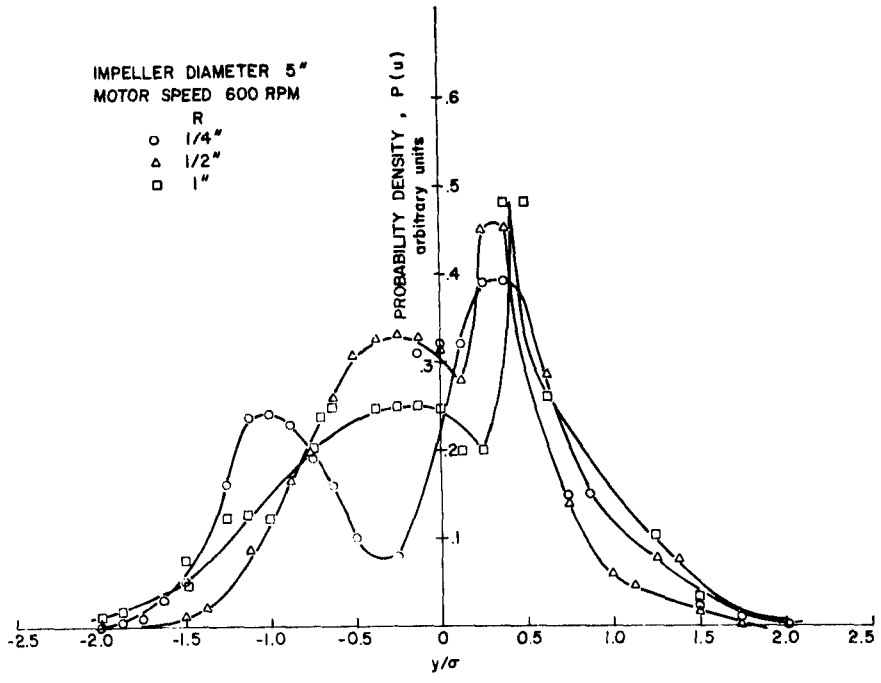

Figure 17 – Probability distribution of radial velocity fluctuations near the impeller tip.

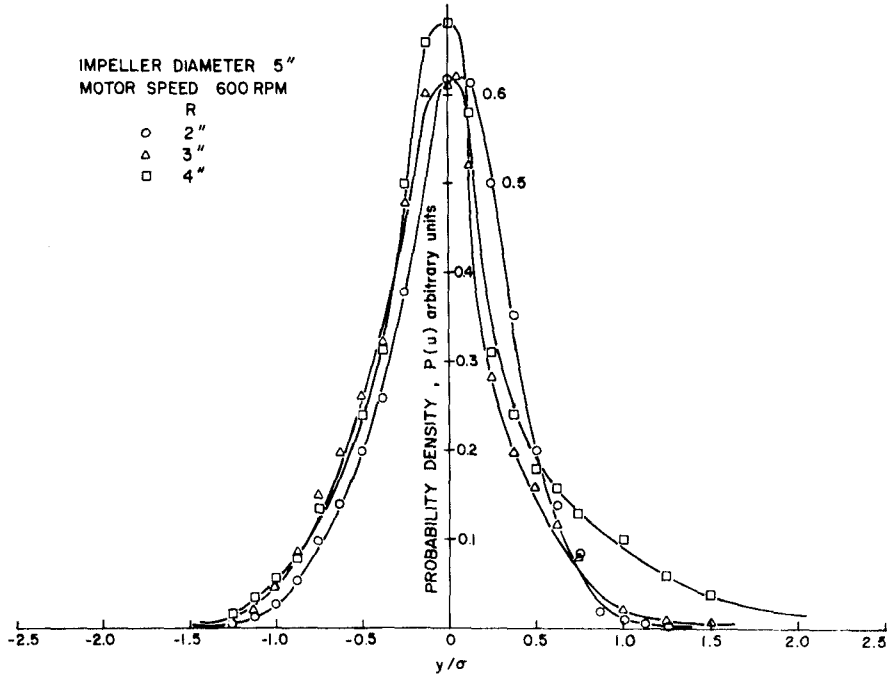

Figure 18 – Probability distribution curves further from the impeller tip.

agree fairly well considering the different methods used. The maximum value of the scale is of the order of the width of the turbine blades (1.0 cm in Cutter's case and 1.3 cm here). This result is consistent with those for grid generated turbulence where the scale is of the order of size of the turbulence generator[28]. However, the scale obtained from the correlation coefficient is much smaller than that from the spectrum, showing that the correlation is heavily biased by the periodic fluctuation. Therefore, this method is unreliable for estimating the integral scale.

The scale of the smallest eddies was calculated from Equation (7). Figures 12 and 13 show a maximum in the range 150-200 Hz yielding a dissipation scale of the 0.1 to 0.2 cm, about ⅕ to 1/10 the size of the spectrum integral scale. It was not possible to obtain Taylor's microscale from the correlation coefficient due to the presence of the periodic component or from the second moment of the spectrum as the data were not analyzed beyond 1000 Hz. A Reynolds number, Re_T, formed from the dissipation scale and u', yields values in the range 40-120. Since less than one decade of Kolmogoroff range would be expected at $Re_T \approx 100$, it is not surprising that an extensive range was not found[27].

Probability density functions

The probability density function of the fluctuating velocity is shown at several radial positions in Figures 17 and 18. Near the impeller (Figure 17) the function has a peak on either side of the mean suggesting the presence of a large periodic component. Since the probability density for a sinusoidal velocity fluctuation is

$$P(u) = \frac{1}{\pi A \sqrt{1 - \frac{1}{2}\left(\frac{u}{\sigma}\right)^2}} \quad \ldots\ldots\ldots\ldots (12)$$

the lower values at $u/\sigma = 0$ are not surprising. The fact that the peaks are not symmetrically placed suggests that the periodic component is not symmetric with respect to the mean fluctuating velocity. Figure 18 shows that as distance from the impeller increases the probability density function becomes more bell-shaped — typical of homogeneous and isotropic turbulence.

A significant implication of the shape observed for the probability density functions is that the technique used by Manning and Wilhelm[13] cannot yield correct values for the microscales since the fluctuating velocity is not distributed normally.

Summary

Since it now appears that similarity of conditions may be assumed for liquids and gases in a stirred tank at equal Reynolds numbers, various turbulence properties were measured in the impeller stream flow of a stirred tank using air as the fluid medium. Because of the large periodic component in velocities near the impeller, there is a large correction which must be made to the intensities of turbulence as usually calculated. The intensities of turbulence, appropriately corrected to eliminate the effect of the periodicity in the mean flow, show a rapid increase from a level of about 5-8% near the impeller tip, to about 35% at a position ⅓ the distance from the impeller tip to the wall. By contrast, the intensities uncorrected for periodicity remain approximately constant at levels of 25-40% over the same range of locations. However, further yet from the impeller tip, the uncorrected intensities also increase with distance, the values reaching about 60% intensity at a position ¾ the distance to the wall. For the corrected intensities, comparison with the 3% level of turbulence intensity which exists at the centerline in turbulent pipe flow emphasizes how highly turbulent the flow conditions are in the impeller stream of an agitated tank.

The energy spectra and the dissipation spectra show large peaks at the impeller-passing frequency and again at higher frequencies. The macroscale, Λ_R, computed from the correlation coefficient was found to be in the range 0.4-1.3 cm., or of the same order as the width of the turbine blades which generate the turbulence. The dissipation scale was in the range 0.1-0.2 cm.

The probability density functions were found to be far from Gaussian, a finding which invalidates earlier published values for the Taylor microscale in stirred tanks.

The measurement by hot-wire anemometry of a number of turbulence properties not previously available has opened a new approach to the study of stirred tanks. Extensive study of the microscopic turbulence structure in stirred tanks is needed, and is being continued in our laboratory.

Acknowledgments

The assistance of E. Koller of The Pulp and Paper Research Institute of Canada in digitizing the data is gratefully acknowledged.

Nomenclature

D = impeller diameter, cm.
R = distance measured radially from tip of impeller, cm.
Re_T = turbulence Reynolds number $Re_T = \frac{u'\lambda}{\upsilon}$
$E_1(k_1)$ = one-dimensional energy spectrum of turbulence in wave number space
k_1 = wave number (in radial direction)
I = intensity of turbulence ($= u'/\overline{U}$)
u' = root-mean-square fluctuating velocity ($= \sqrt{\overline{u^2}}$)
$\overline{U}$ = local mean velocity, cm/sec
k_d = Kolmogoroff wave number, cm^{-1}
f = frequency, Hz
U_c = convection velocity, cm/sec.
$R(\tau)$ = auto-correlation function $\left(= \frac{\overline{u(t)u(t+\tau)}}{\overline{u^2}} \right)$
$P(u)$ = amplitude probability density function for turbulent velocity fluctuations (PDF)
f_t = turbulence generating frequency, Hz
U_{TIP} = impeller tip velocity $= \pi DN$
r = radial distance measured from the center line of the tank
N = impeller speed, rpm
A = amplitude of periodic component
n_b = number of blades on turbine
K = r.m.s. value of random noise
y = amplitude of velocity signal recorded on strip chart

Greek Symbols

υ = kinematic viscosity
ρ = $1 + 2R/D$; dimensionless distance from the center line of tank
α = noise time correlation constant, $msec^{-1}$
ω = angular frequency ($= 2\pi f$)
ϵ = energy dissipation per unit mass
Λ = integral scale of turbulence, cm.
λ = Taylor micro-scale of turbulence, cm.
τ = time delay, msec

Subscripts

R = derived from auto-correlation function
E = derived from energy spectrum

References

(1) Cooper, R. G., M. Eng. Thesis, McGill Univ., Montreal (1966).
(2) Chuang, H. and Cermak, J. E., AIChE Journal, 13, 266 (1967).
(3) Sandborn, V. A., NACA Tech. Note 3266 (1955).
(4) Laufer, J., NACA Tech. Note 2954 (1953).
(5) Martin, G. Q. and Johanson, L. N., AIChE Journal, 11, 30 (1965).
(6) Wells, C. S., Harkness, J. and Meyer, W. A., Rept. No. 0-71000/6R-22, LTV Research Center, Dallas, Texas (1966).
(7) Fabula, A. G., Rept. to U.S. Bureau of Naval Weapons, Under Contract No. (G)-00043-65. Department of Aeronautical Engineering, The Pennsylvania State University (1966).
(8) Rosler, R. S. and Bankoff, S. G., Rev. Sci. Instr., 33 ,1209 (1962).
(9) Rosler, R. S. and Bankoff, S. G., AIChE Journal, 9, 672 (1963).
(10) Corrsin, S. NACA WR, W-94 (1943).
(11) Corrsin, S. and Uberoi, M. S., NACA Rept., 998 (1950).
(12) Comte-Bellot, G. and Corrsin, S., Unpublished, Johns Hopkins University, Md., Quoted in Fabula (7).
(13) Manning, F. S. and Wilhelm, R. H., AIChE Journal, 9, 12 (1963).
(14) Rieth, T., Proc. AIChE-IChemE Joint Meeting; London (1965) Symposium No. 10, 14 (1965).
(15) Kim, W. J. and Manning, F. S., AIChE Journal, 10, 747 (1964).
(16) Bowers, R. H., Proc. AIChE-IChemE Joint Meeting; London (1965).
(17) Schwartzberg, H. G. and Treybal, R. E., Ind. Eng. Chem. Fundamentals 7, 1 (1968).
(18) Cutter, L. A., AIChE Journal, 12, 35 (1966).
(19) Cutter, L. A., Paper presented at the 17th Canadian Chemical Engineering Conference, Windsor (1967).
(20) Kolmogoroff, A. N., Comp. Rend. Acad. Sci. URSS (Doklady), 30 4 (1941).
(21) Hinze, J. O., "Turbulence", McGraw-Hill Book Co., New York (1959).
(22) Townsend, A. A., "Structure of Turbulent Shear Flows", Cambridge Univ. Press (1956).
(23) Fisher, M. J. and Davies, P. O. A. L., J. Fluid Mech. 18, 97 (1963).
(24) Rust, J. H. and Sesonske, A., Int. J. Heat Mass Transfer, 9, 215 (1966).
(25) Davies, P. O. A. L., AIAA Journal, 4, 1971 (1966).
(26) Snyder, W. H. and Margolis, D. P., Phys. Fluids, 10, 963 (1967).
(27) Grant, H. L., Stewart, R. W. and Moillet, A., J. Fluid Mech. 12, 241 (1962).
(28) Uberoi, M. S. and Corrsin, S., NACA Rept. 1142 (1953).

Manuscript received November 28, 1968; accepted March 31, 1970.
Based on a paper presented to the 1968 Tripartite Chemical Engineering Conference, Montreal, Quebec, September 22-25, 1968.

★ ★ ★